4208 *Biochemistry* **2010,** *49,* 4208–4219
DOI: 10.1021/bi100330w

BIOCHEMISTRY
including biophysical chemistry & molecular biology
Article

Molecular Cloning of the Human Platelet-Derived Growth Factor Receptor β (PDGFR-β) Promoter and Drug Targeting of the G-Quadruplex-Forming Region To Repress PDGFR-β Expression[†]

Yong Qin,[‡] Jessica S. Fortin,[‡] Denise Tye,[‡] Mary Gleason-Guzman,[‡] Tracy A. Brooks,[‡,§,∥] and Laurence H. Hurley*[,‡,§,∥,⊥]

[‡]*College of Pharmacy, 1703 East Mabel, University of Arizona, Tucson, Arizona 85721,* [§]*Arizona Cancer Center, 1515 North Campbell Avenue, Tucson, Arizona 85724,* [∥]*BIO5 Collaborative Research Institute, 1657 East Helen Street, Tucson, Arizona 85721, and* [⊥]*Department of Chemistry, University of Arizona, Tucson, Arizona 85721*

Received March 4, 2010; Revised Manuscript Received April 7, 2010

ABSTRACT: To understand the mechanisms controlling platelet-derived growth factor receptor β (PDGFR-β) expression in malignancies, we have cloned and characterized the first functional promoter of the human PDGFR-β gene, which has been confirmed by luciferase reporter gene assays. The transcription initiation sites were mapped by primer extension. Promoter deletion experiments demonstrate that the proximal, highly GC-rich region (positions −165 to −139) of the human PDGFR-β promoter is crucial for basal promoter activity. This region is sensitive to S1 nuclease and likely to assume a non-B-form DNA secondary structure within the supercoiled plasmid. The G-rich strand in this region contains a series of runs of three or more guanines that can form multiple different G-quadruplex structures, which have been subsequently assessed by circular dichroism. A *Taq* polymerase stop assay has shown that three different G-quadruplex-interactive drugs can each selectively stabilize different G-quadruplex structures of the human PDGFR-β promoter. However, in transfection experiments, only telomestatin significantly reduced the human PDGFR-β basal promoter activity relative to the control. Furthermore, the PDGFR-β mRNA level in Daoy cells was significantly decreased after treatment with 1 μM telomestatin for 24 h. Therefore, we propose that ligand-mediated stabilization of specific G-quadruplex structures in the human PDGFR-β promoter can modulate its transcription.

PDGF dimers AA, AB, BB, CC, and DD exert their cellular effects through two tyrosine kinase α- and β-receptors (*1*, *2*). The PDGFR-β[1] signaling pathway is an essential component in the control of the growth, survival, motility, and differentiation of cells, particularly connective tissue (*2*, *3*). Overactivity of PDGF dimer BB or PDGFR-β contributes to the development of certain diseases characterized by excessive cell growth, including fibrotic disorders, atherosclerosis, and malignancies (*2*, *3*). In solid tumors, PDGFR-β signaling participates in various processes, including autocrine stimulation of tumor cell growth, recruitment of tumor stroma fibroblasts, angiogenesis, metastasis, and the increase in interstitial fluid pressure (*3*−*6*). The PDGFR-β signaling pathway has been implicated as an important therapeutic target for cancer treatment and evaluated in different animal disease models, as well as in clinical trials (*6*−*8*). A study of the B16 mouse melanoma tumor model has shown that the increased tumor growth rate associated with PDGF dimer DD production was not seen in mice expressing attenuated PDGFR-β and was thus dependent on the host PDGFR-β signaling pathway (*9*). Therefore, the down-regulation of PDGFR-β expression in tumor cells is predicted to reduce the cellular response to PDGF dimer BB or DD, resulting in inhibition of tumor growth.

For most genes, transcriptional initiation is the key step for gene expression. Dysfunction in transcriptional initiation causes abnormal gene expression. An essential requirement for understanding deregulation of gene expression in the disease process is a comprehensive knowledge of the sequence of the gene promoter, since this determines the combinatorial control of gene expression by different transcriptional factors. The mouse PDGFR-β promoter has been isolated and thoroughly characterized (*10*−*12*). Multiple transcription factors have been found that bind to this promoter and regulate mouse PDGFR-β expression, such as Sp1, c-Myc, p73α, p53, NF-Y, and Arf (*12*−*19*). However, the functional promoter of human PDGFR-β has not been cloned or characterized, and consequently, the molecular mechanisms governing the transcription of the human PDGFR-β gene are not understood.

For these reasons, we have cloned the human PDGFR-β promoter and initiated characterization of this promoter. An important S1 nuclease hypersensitive region that responds to human PDGFR-β activation has been identified. This S1-sensitive region can form multiple G-quadruplex structures. It has been shown that tandem repeats of the G-tract sequence can adopt intramolecular G-quadruplex structures in the promoters of several important human genes, such as c-Myc, Bcl-2, VEGF, HIF-1α, RET, c-Kit-1, c-Kit-2, c-Myb, KRAS, PDGF-A, and hTERT (*20*−*34*). We have also demonstrated that G-quadruplexes formed in the human PDGFR-β promoter can be

[†]This research has been supported by grants from the National Institutes of Health (GM085585-01 and CA95060) and the Arizona Biomedical Research Commission (9006).

*To whom correspondence should be addressed. Telephone: (520) 626-5622. Fax: (520) 626-0035. E-mail: hurley@pharmacy.arizona.edu.

[1]Abbreviations: PDGFR-β, platelet-derived growth factor receptor β; PCR, polymerase chain reaction; CD, circular dichroism; AP-1, activator protein 1; NHE, nuclease hypersensitive element; LUC, luciferase reporter gene.

 Published on Web 04/08/2010

targeted by the G-quadruplex-interactive molecule telomestatin, which has been shown to have an inhibitory effect on human PDGFR-β promoter activity in both plasmid transfection experiments and human cancer cells. These results also demonstrate that the mechanism of action of telomestatin in cells is not restricted to targeting telomeric G-quadruplexes but is likely mediated through G-quadruplexes in promoter regions, such as hTERT (*32*) and PDGFR-β, as well as through alterations in splicing sites in the hTERT region (*35*).

MATERIALS AND METHODS

Materials. DNA oligomers were obtained from Biosearch Technologies, Inc. An acrylamide/bisacrylamide (29:1) solution and ammonium persulfate were purchased from Bio-Rad, and *N*,*N*,*N*′,*N*′-tetramethylethylenediamine was purchased from Fisher. T4 polynucleotide kinase and *Taq* DNA polymerase were purchased from Promega. [γ-^{32}P]ATP was purchased from NEN Dupont. TMPyP2, TMPyP4, and Se2SAP were synthesized in our laboratory. Telomestatin was kindly provided by K. Shin-ya (University of Tokyo, Tokyo, Japan). Plasmid pGL3-basic, pRL-TK, and dual luciferase assay kits were purchased from Promega.

Cloning of the Human PDGFR-β Promoter and Plasmid Construction. Human genomic DNA was purified from human HPDE-6 cells and used as a template for PCR. Two primers (5′-CCCAGTTATCAGAAAGACTGC-3′ and 5′-GCCAGCCTCTACCTGTGTCAC-3′) were designed to amplify a 2097 bp fragment of the 5′-flanking region of the human PDGFR-β gene. This fragment comprises 1724 bp in the 5′-flanking region and the adjacent 373 bp located at the 5′-end of the first exon of human PDGFR-β. The 2097 bp DNA fragment was cloned into the Topo-TA cloning vector (Invitrogen) to generate plasmid construct hPRB-Topo-2kb for further study. Five designed primers (5′-TGCACCCGGTACCGTGTTAG-3′, 5′-GGCAGGGGGTACCTCTACAC-3′, 5′-CCTTCTCCCAGCTAGCCCAATCAG-3′, 5′-GGAGGGAGCTAGCAGAGTG-3′, and 5′-GTGCCATGGCTAGCGGAGGC-3′), which contain restriction enzyme sites, were paired with the same reverse primer (5′-TGGGCAGCTCGAGCACAGGC-3′) to amplify different deleted constructs (256, 380, 531, 672, and 1215 bp) of the human PDGFR-β promoter from hPRB-Topo-2kb. We used the pGL3-basic promoter−reporter fusion system to analyze the promoter function of these genomic DNA fragments. These human PDGFR-β promoter fragments were subcloned into the XhoI−KpnI or XhoI−NheI restriction sites of the pGL3-basic vector to produce plasmid constructs pGL-A, pGL-B, pGL-C, pGL-D, and pGL-E.

Primer Extension. Approximately 1×10^6 cpm of ^{32}P-labeled primer PEX56 (5′-TCTCTGGCTCCAAGTTGCTCAC-3′), complementary to the first exon of PDGFR-β genomic DNA (positions 20−41), was annealed to 1.5 μg of human mRNA isolated from Daoy cells when the reaction mixture was heated to 90 °C for 2 min and cooled to 55 °C over 1 h. Primer extension analysis was performed using a standard protocol (*36*). A sequencing reaction for determining the position of the primer extension product was performed with a Thermo Sequenase Cycle Sequencing Kit (USB) according to the manufacturer's protocol. Primer PEX56 was also used for the sequencing reaction with plasmid template hPRB-Topo-2kb.

S1 Nuclease Sensitivity Assay. Plasmids pGL-B and pGL-E were incubated with S1 nuclease (1 unit of S1 nuclease per microgram of plasmid) for 5 min at 37 °C. Digested plasmid DNA was extracted with phenol and a chloroform/isoamyl alcohol mixture, precipitated with 100% ethanol, and resuspended in doubly distilled water after being vacuum dried. To map the S1 nuclease cleavage site, the nicked plasmid was PCR-amplified using ^{32}P-labeled sequencing primers RV3 and GL2 for the pGL3-basic vector (Promega) and a Thermo Sequenase Cycle Sequencing Kit (USB).

CD Spectroscopy. CD spectra were recorded on a J-810 spectropolarimeter (Jasco, Easton, MD) using a quartz cell with an optical path length of of 1 mm and an instrument scanning speed of 100 nm/min, with a response time of 1 s, over a wavelength range of 200−330 nm. All DNA samples were dissolved and diluted in Tris-HCl buffer (50 mM, pH 7.4), and where appropriate, the samples also contained different concentrations of KCl and/or NaCl. The DNA strand concentrations were 5 μM, and the CD data represent four averaged scans taken at room temperature. All CD spectra were baseline-corrected for signal contributions due to the buffer.

Labeling and Purification of Oligodeoxyribonucleotides. The DNA oligomers were 5′-end-labeled with [γ-^{32}P]ATP using T4 polynucleotide kinase for 1 h at 37 °C. The labeling reaction was stopped when the samples were heated at 90 °C for 8 min after the addition of 1.5 μL of 0.5 M EDTA. The 5′-end-labeled DNA was then purified using a Bio-Spin 6 chromatography column (Bio-Rad). The labeled DNA was further purified by running a 12% denatured polyacrylamide gel that contained 8.0 M urea.

Taq Polymerase Stop Assay. The DNA primer 5′-TCGACTCTAAGCAAATGCGTCGAG-3′ labeled at the 5′-end with ^{32}P was annealed to the DNA template (5′-GCTGGGAGAAGGGGGGGCGGCGGGGCAGGGAGGGTGGATTAGTCAGACCTCGACGCATTTGCTTAGAGTCGA-3′) and subjected to the *Taq* polymerase stop assay based on the same protocol found in ref *37*.

DMS Footprinting. The 100000 cpm of DNA samples labeled at the 5′-end with ^{32}P was preincubated in different salt buffers or treated with different drugs at room temperature for 30 min before DMS footprinting. The procedure for DMS footprinting has been described in refs *21* and *31*.

Imaging and Quantitation. The dried gel was exposed on a phosphor screen. Imaging and quantitation were performed using a Storm 820 phosphorimager and ImageQuant version 5.1 from Molecular Dynamics.

Cell Culture and DNA and RNA Isolation. Human normal pancreatic cell line HPDE-6 was cultured in keratinocyte-SFM medium containing 100 units/mL penicillin, 100 μg/mL streptomycin, 200 mM L-glutamine, bovine pituitary extract, epidermal growth factor, and 10% FBS (GIBCO). Human medulloblastoma Daoy cells (ATCC) were cultured in Eagle's minimum essential medium containing 100 units/mL penicillin, 100 μg/mL streptomycin, 200 mM L-glutamine, and 10% FBS at 37 °C in a humidified atmosphere of 95% air and 5% CO_2. Cells were maintained in a logarithmic phase of growth. The isolation of total cellular DNA was conducted with cells at subconfluency using a NucleoSpin DNA Kit (Macherey-Nagel), and the total cellular RNA was extracted using a NucleoSpin RNA II Kit (Macherey-Nagel).

Cell Transient Transfection and Dual Luciferase Assay. For transfection experiments, Daoy cells were seeded in six-well dishes with a concentration of 2×10^5 cells per well and cultured at 37 °C (in a humidified atmosphere of 95% air and 5% CO_2) for 24 h before drug treatment. Each well was cotransfected with 2 μg

of constructed plasmids and 25 ng of pRL-TK with Lipofectin (Invitrogen). pRL-TK (Promega), containing a Renilla luciferase gene driven by the herpes simplex virus thymidine kinase promoter, was used as a control for transfection efficiency. The pGL3 promoter vector was used as a positive control of luciferase expression. The level of expression of firefly luciferase, with respect to that of Renilla luciferase, was determined using a dual luciferase assay kit (Promega) 24 h after transfection (according to the manufacturer's directions). Cell lysate (20 μL) was mixed with 100 μL of reconstituted luciferase assay reagent, and light output was measured for 12 s with an FB12 luminometer (Berthold). To test the effects of G-quadruplex-interactive agents on human PDGFR-β promoter activity, varying concentrations of telomestatin, Se2SAP, TMPyP4, or TMPyP2 (up to 50 μM) were cotransfected with the constructed plasmid (pGL-A) and pRL-TK into Daoy cells. The cells were then subjected to the dual luciferase assay after drug treatment for 24 h.

Reverse Transcriptase Polymerase Chain Reaction. To check the mRNA level of PDGFR-β in Daoy cells, the first-strand cDNA synthesis was performed with 200 ng of total RNA by using the iScript cDNA Synthesis Kit (Bio-Rad). In a 25 μL reaction mixture, a 1 μL cDNA product was used for each PCR in the presence of 4 mM $MgCl_2$, 0.1 mM dNTPs, and 2.5 units of *Taq* polymerase (Promega). The primers 5′-AATGTCTCCAG-CACCTTCGT-3′ and 5′-AGCGGATGTGGTAAGGCATA-3′ were used to PCR-amplify a 688 bp fragment of human PDGFR-β cDNA (*38*). Primers 5′-CCACCCATGGCAAATTCCATGG-CA-3′ and 5′-TCTAGACGGCAGGTCAGGTCCACC-3′ were used to amplify a 600 bp fragment of human glyceraldehyde-3-phosphate dehydrogenase (GAPDH) cDNA (*39*). The PCR protocol was as follows: initial denaturation at 95 °C for 5 min; 30 cycles of 95 °C for 40 s, 50.5 °C for 30 s, and 72 °C for 60 s; primer extension at 72 °C for 1 min; and a final extension at 72 °C for 10 min. Fifteen microliters of PCR product was analyzed on a 1% agarose gel.

RESULTS

Functional Promoter Region of Human PDGFR-β. The human PDGFR-β gene is located on chromosome 5q33, and the coding region for its pre-mRNA consists of ~5.5 kb (refs *40* and *41*, and as shown in the NCBI GenBank). Typically, the promoter is located in the 5′-flanking region of the first exon of the gene. Therefore, we used the 470 bp 5′-end cDNA sequence of human PDGFR-β (GenBank accession number BC032224) in a BLAST search of the human genome to determine the DNA sequence of this region (Figure 1A). Primers (underlined in Figure 1A) were designed to amplify each of the five overlapping DNA fragments in the 5′-flanking region [1215 (−1099 to 116), 672 (−556 to 116), 531 (−415 to 116), 380 (−264 to 116), and 256 (−140 to 116) bp]. Each of these constructs contains different lengths of the human PDGFR-β promoter region and a 116 bp human PDGFR-β coding sequence downstream of the major transcription start site, which was determined by a primer extension assay. All five fragments were confirmed to be 100% identical with the human genome sequence, shown by double-strand DNA sequencing. Luciferase reporter constructs were generated by insertion of each of these five fragments into the pGL-3-basic vector in the same orientation in which they drive the expression of human PDGFR-β. These plasmid constructs were designated pGL-A, pGL-B, pGL-C, pGL-D, and pGL-E (Figure 1B, top).

These constructs were each subjected to a transient cotransfection assay with pRL-TK in Daoy cells, in which the PDGFR-β mRNA is strongly expressed. The promoter activities of these five reporter constructs in Daoy cells are shown in Figure 1B (bottom) as the fold increase in reporter firefly luciferase activity relative to internal control Renilla luciferase activity. All the constructs exhibited a significant increase in luciferase activity over the negative control, pGL-3-basic ($P < 0.001$) (Figure 1B, bottom). This confirmed that we had cloned the functional promoter region of human PDGFR-β. The minimal functional fragment of the human PDGFR-β promoter, which is responsible for the basal promoter activity, was determined to be the region of base pairs −140 to 116 in pGL-A. pGL-B (base pairs −264 to 116) has a 2-fold increase in promoter activity over pGL-A, indicating that there are essential regulatory elements located within the region of base pairs −264 to −140. The similar promoter activities of pGL-B and pGL-C (base pairs −415 to 116) suggest that there may not be any important *cis* elements within the region of base pairs −264 to −415. However, the significant increase in the promoter activity of pGL-D (base pairs −556 to 116) implies the presence of enhancing elements within the region of base pairs −415 to −556. The highest promoter activity is seen with the −1099 to 116 construct (pGL-E), indicating the existence of important positive *cis* elements within the region of base pairs −1099 to −556.

Gene2Promoter (Genomatix Software Inc.) was used to identify the homologues to well-known *cis* elements within the human PDGFR-β promoter. Two conserved binding sites for activator protein 1 (AP-1) at base pairs −342 to −336 and −494 to −488 (-AGTCAct- in the antisense strand), two conserved Sp1 binding sites at base pairs −152 to −147 (-GGCGGG- sequence in the antisense strand) and base pairs −87 to −82 (-GGCGGG- sequence in the sense strand), and one conserved NFE2 binding site (-gctgAGTCAct-) overlapping with one of the AP-1 binding sites at base pairs −342 to −336 were identified in the human PDGFR-β promoter (Figure 1A). While there is no classical TATA box in the human PDGFR-β promoter, a consensus CAAT box (GGNCAATC) has been identified at base pairs −126 to −119, which is also the conserved binding site for NF-Y. The CAAT box (base pairs −126 to −119) and Sp1 binding sites (base pairs −87 to −82) may play critical roles in determining the basal promoter activity of human PDGFR-β observed in pGL-A. The Sp1 binding site (base pairs −152 to −147) located within the polypurine/polypyrimidine sequence (base pairs −165 to −132) contains a series of contiguous G-tracts in the G-rich strand. A significant increase in promoter activity in pGL-B over pGL-A indicates that this polypurine/polypyrimidine region plays a critical role in regulating human PDGFR-β transcription. Additionally, two conserved NF-Y binding sites were also found at base pairs −849 to −845 and −802 to −798 (Figure 1A), which may contribute to the strong promoter activity observed in pGL-E (Figure 1B, bottom).

A specific primer, PEX56 (as described in Primer Extension), that is complementary to human PDGFR-β mRNA was used to identify the transcription start site(s) in the primer extension analysis. The primer extension along the total mRNA of Daoy cells generates a predominant band, which corresponds to the guanine residue (sense strand) located 171 nucleotides upstream of the ATG start codon and is predicted to be the major transcription start site (Figure 1C). A weaker primer extension product located at the thymine residue (sense strand) 160 nucleotides upstream of the ATG codon was also observed (Figure 1C). Thus, transcription of human PDGFR-β may

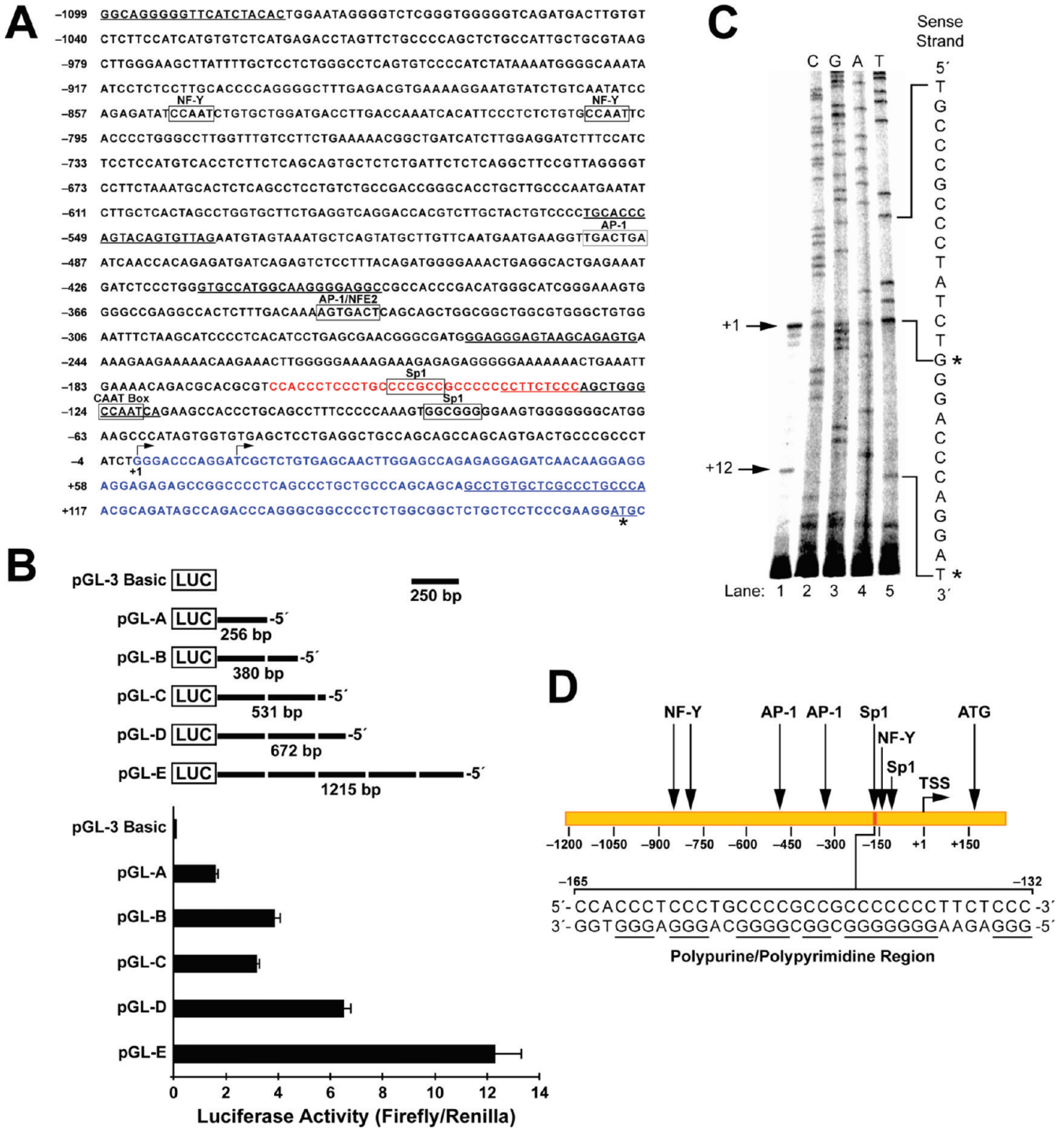

FIGURE 1: (A) DNA sequence of the 5′-flanking region of the human PDGFR-β gene. The 3′-end sequence of exon 1 is colored blue. The putative *cis* elements in the human PDGFR-β promoter are boxed. Arrows indicate the locations of the two transcription start sites, and the major transcription start site is numbered +1. The ATG start codon is marked by an asterisk at the 3′-end. The sequences of primers that amplify different lengths of human PDGFR-β promoter are underlined. The important polypurine/polypyrimidine region in the proximal promoter is colored red. (B) Promoter−luciferase−reporter constructs containing the indicated region of the human PDGFR-β promoter and 5′-UTR (LUC = luciferase reporter gene) (top). Deletion analysis of human PDGFR-β promoter activity showing the comparative firefly luciferase expression (firefly/Renilla) of each plasmid construct presented as a bar graph (bottom). The promoter-less construct pGL-3-basic serves as a negative control. The values are the averages of three independent experiments (error bars are the standard errors). (C) Identification of transcription start sites of the human PDGFR-β gene by primer extension. Lane 1 shows primer extension by PEX56 using the human PDGFR-β mRNA as a template. The transcriptional start sites are shown by arrows to the left of this lane. Lanes 2−5 show sequencing reactions on the sense strand of the human PDGFR-β promoter loaded in the order CGAT. The bases corresponding to the two transcription start sites are indicated on the sequence at the right of the gel by asterisks. (D) Diagram of the human PDGFR-β promoter and location of important putative *cis* elements. The polypurine/polypyrimidine region is shown in the inset, and the important G-tracts are underlined.

start at two sites, located either 171 or 160 nucleotides upstream of the start codon. The major transcription start site is denoted as +1, and upstream bases are then numbered negatively. On the basis of our study, a model showing the organization of the human PDGFR-β promoter and the locations of putative transcription factor binding sites is proposed (Figure 1D).

The C-Rich Strand of the Polypurine/Polypyrimidine Region in the Human PDGFR-β Promoter Is Sensitive to S1 Nuclease. The DNA region that is sensitive to endonuclease DNase I and/or S1 usually assumes non-B-form DNA structures and contains important *cis* elements within the chromatin (*42*−*44*). Therefore, we tested the S1 nuclease sensitivity of the human PDGFR-β promoter by digesting plasmids pGL-E and pGL-B with S1 nuclease. One particularly S1-sensitive region consistently appeared within the polypurine/polypyrimidine region (base pairs −132 to −165) of the human PDGFR-β promoter in both plasmids. Fine mapping of this region in pGL-B showed that the major S1-hypersensitive sites lay predominantly within four cytosine tracts (base pairs −158 to −139) of the cytosine-rich (C-rich) sense strand in the human PDGFR-β promoter (Figure 2, lanes 3 and 4). Significantly, there was no strong S1 nuclease cleavage site detected on the G-rich strand in a very broad region (base pairs 1−1000) under the same experimental conditions for S1 digestion (data not shown). This indicates that the G-rich strand of the PDGFR-β promoter is far less sensitive than the C-rich strand. Consequently, we have designated the polypurine/polypyrimidine region (base pairs −165 to −132) as the nuclease hypersensitive element (NHE). The preferential cleavage of the C-rich strand of NHE by S1 nuclease indicates that the NHE under supercoiled torsional stress assumes a paranemic DNA structure, in which the C-rich strand retains a single-stranded conformation that is sensitive to S1 nuclease, whereas the NHE G-rich strand most likely forms a DNA secondary structure that is resistant to S1 nuclease.

CD Spectroscopy Shows That the G-Rich Strand of the NHE Forms G-Quadruplex Structures. It has been shown that tandem repeats of the G-tract sequence can adopt intramolecular G-quadruplex structures in the promoters of several important genes, such as c-Myc, Bcl-2, VEGF, HIF-1α, RET, c-Kit-1, c-Kit-2, c-Myb, KRAS, PDGF-A, and hTERT (*20*−*33*). The G-rich strand of the NHE in the human PDGFR-β promoter contains five guanine runs of three or more contiguous bases, each separated by four, four, two, and one base(s) from the 5′-end, respectively (sequence shown in Figure 1D). By analogy with the G-quadruplex-forming region of other promoters, the G-rich strand of the NHE has the potential to form one or more three-tetrad G-quadruplex structures under physiological conditions.

CD spectroscopy has been well established to determine the existence and infer the topology of G-quadruplex structures in a DNA sequence (*45*). Therefore, the DNA oligomer NHE Pu38-mer, which contains the whole core sequence of the G-rich strand of NHE, was subjected to CD in the presence of KCl and NaCl (sequence shown in Figure 3A). Figure 3A shows that in the presence of 100 mM KCl, the NHE Pu38-mer exhibits a CD spectrum (red line) characterized by a maximum positive ellipticity at 265 nm, a negative band at 240 nm, and a minor positive band at 212 nm, suggesting that it assumes primarily a parallel G-quadruplex structure in KCl. In 100 mM NaCl, the CD spectrum of the NHE Pu38-mer (Figure 3A, black line) has pronounced shoulder absorption between 280 and 300 nm, which is the characteristic signature of a mixed parallel/antiparallel G-quadruplex structure (*22*, *46*). KCl and NaCl can both dramatically increase the elliptic intensity of NHE Pu38-mer CD spectra, indicating that alkali metal ions can facilitate the formation of G-quadruplexes in this sequence. The change in Tm was also measured as an indication of stabilization. In the absence of any salt, the T_m of the NHE Pu38-mer is 36 °C. In the presence of either NaCl or KCl, the melting temperature of the parallel positive peak is increased to 54 or 73 °C, respectively. Since KCl is the dominant alkali ion under physiological conditions in cells (~140 mM KCl and 5−10 mM NaCl) (*47*, *48*), the major PDGFR-β NHE G-quadruplex in cells is likely to be a largely parallel structure.

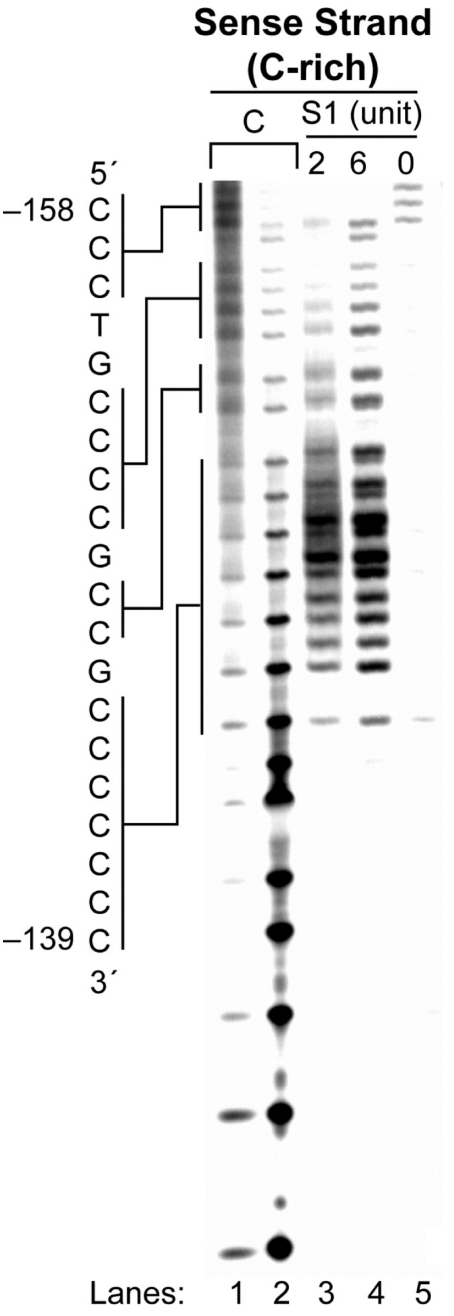

FIGURE 2: Identification of S1 nuclease hypersensitive sites in the human PDGFR-β proximal promoter. Lanes 1 and 2 show the cytosine sequencing reactions on the sense strand (C-rich strand). Plasmid pGL-B was pretreated with different amounts of S1 nuclease before PCR (lanes 3 and 4), and the S1 nuclease cleavage sites were mapped by PCR using specific ^{32}P-labeled primers. Lane 5 is the same as lanes 3 and 4 but without S1 nuclease. The sequence and locations of the S1 hypersensitive regions on the C-rich strands are shown to the left of the gel.

KCl Facilitates the Formation of Intramolecular G-Quadruplexes in the G-Rich Strand of the NHE. The specific stabilizing effect of KCl and NaCl on the formation

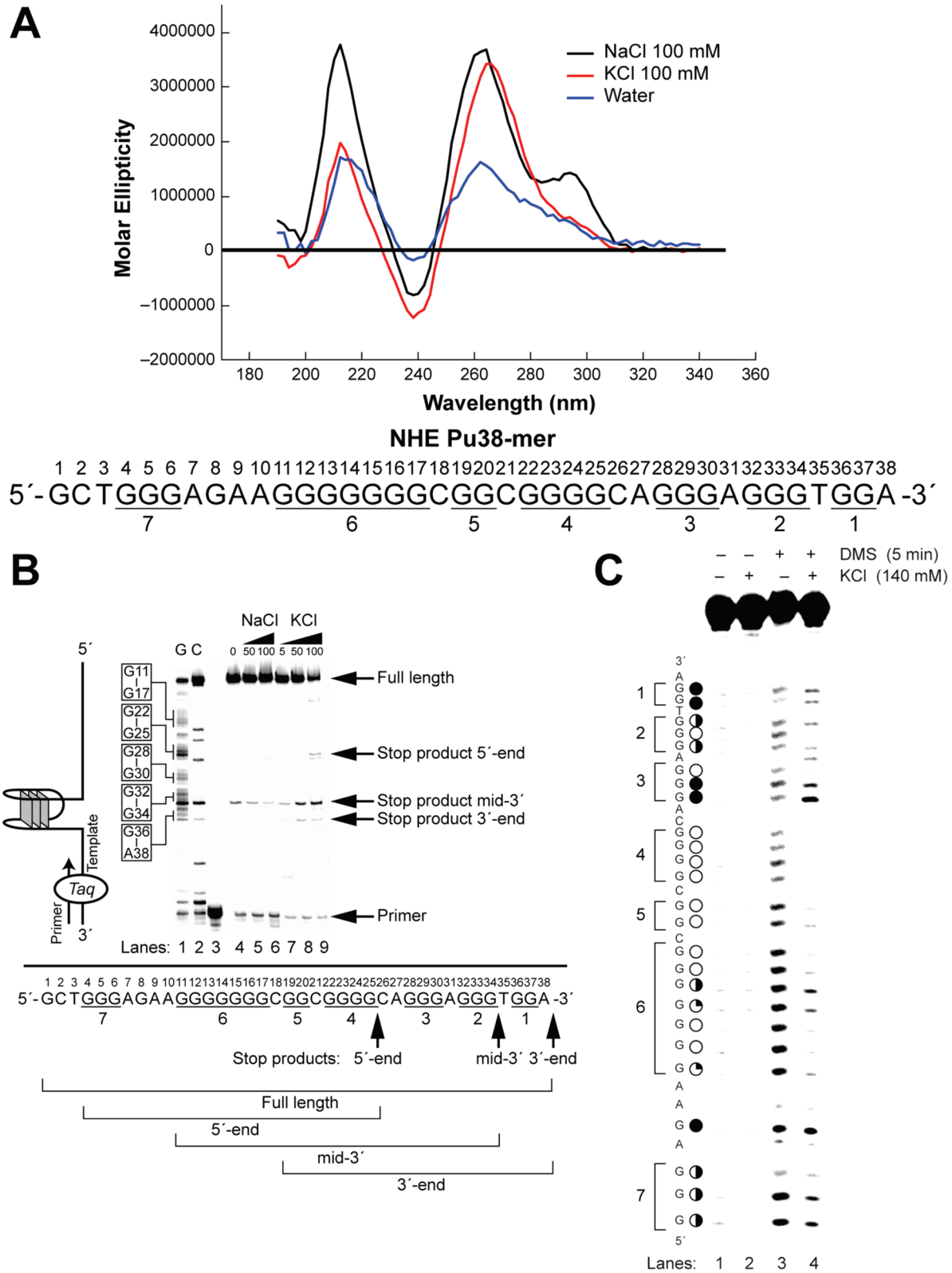

FIGURE 3: (A) Effect of NaCl and KCl on the PDGFR-β NHE Pu38-mer CD spectra. The CD signals of the NHE Pu38-mer in 100 mM NaCl, 100 mM KCl, and water are colored black, red, and blue, respectively. All CD data were obtained with a DNA concentration of 5 μM at 25 °C. The sequence of the NHE Pu38-mer is shown under the CD spectra. (B) Effect of increasing concentrations of NaCl and KCl on the stability of G-quadruplex structures within the NHE Pu38-mer using the *Taq* polymerase stop assay. Lanes 1 and 2 represent the guanine and cytosine sequencing reactions, respectively. Lane 3 is the ^{32}P-labeled primer without *Taq* polymerase. The primer extension reaction in lane 4 was performed in the buffer without KCl or NaCl. The samples in lanes 5−9 were preincubated with different concentrations of KCl or NaCl before the primer extension reaction. The three primer extension stop products are designated 5′-end, mid-3′, and 3′-end. The corresponding sites for the stop products are indicated on the core G-tract sequence of the NHE Pu38-mer at the bottom of the gel. (C) DMS footprinting of intramolecular G-quadruplex structures in the NHE. The NHE Pu38-mer (full length) was incubated in a Tris buffer without KCl (lanes 1 and 3) or in the presence of 140 mM KCl (lanes 2 and 4) before being treated with DMS. The seven runs of two or more guanines are indicated by brackets. DMS methylation patterns are indicated by empty circles (protected), quarter-shaded circles (slightly cleaved), half-shaded circles (partially protected), and fully shaded circles (unprotected).

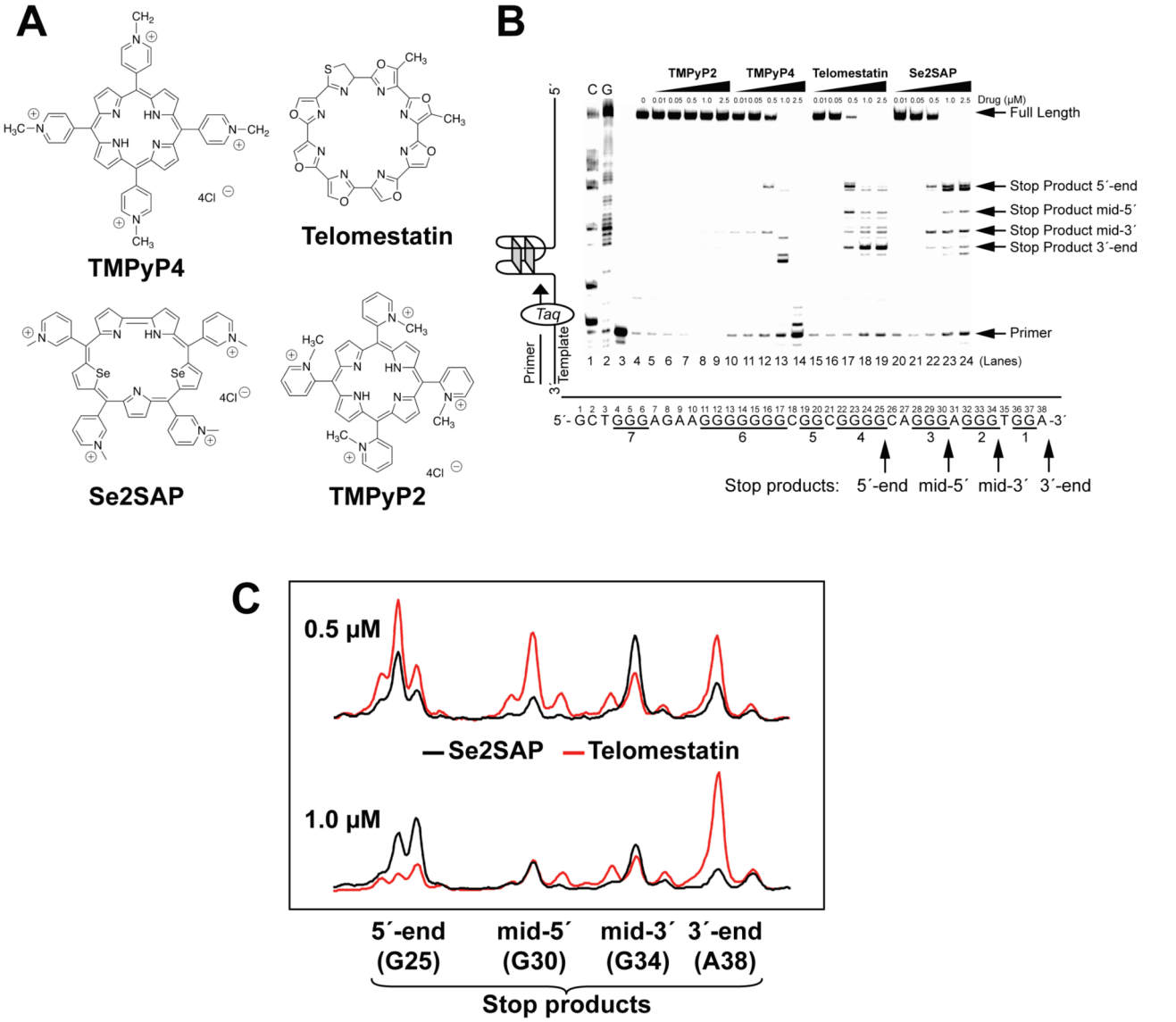

FIGURE 4: (A) Structures of the G-quadruplex-interactive compounds TMPyP4, telomestatin, and Se2SAP and the control compound TMPyP2. (B) The *Taq* polymerase stop assay was used to compare the stabilization of the PDGFR-β NHE G-quadruplex by TMPyP2 (lanes 5−9), TMPyP4 (lanes 10−14), telomestatin (lanes 15−19), and Se2SAP (lanes 20−24) by using increasing concentrations of drugs (0.01, 0.05, 0.5, 1.0, and 2.5 μM) at 60 °C. Lanes 1 and 2 are sequencing reactions on the template. Lane 3 is labeled primer, and lane 4 is without drug. The four primer extension stop products are designated 5′-end, mid-5′, mid-3′, and 3′-end. The corresponding arrest sites are indicated on the core G-tract sequence of the NHE Pu38-mer below the gel. (C) Graphical representation of autoradiograms showing the effects of Se2SAP and telomestatin on the formation of stop products in the *Taq* polymerase stop assay from panel B at concentrations of 0.5 and 1.0 μM.

of G-quadruplexes in the G-rich strand of the NHE was further evaluated by a *Taq* polymerase stop assay (Figure 3B) (*21*, *31*). A cassette template DNA containing the NHE Pu38-mer was annealed with a ^{32}P-labeled primer, which subsequently was extended with *Taq* polymerase under different conditions. In the absence of NaCl or KCl, the major portion of the primer was extended to form a full-length product, and a primary arrest product occurred at G34 (stop product mid-3′) of the NHE Pu38-mer (Figure 3B, lane 4). Upon addition of KCl to the mixture, the level of stop product mid-3′ increased in a KCl-dependent manner (Figure 3A, lanes 8 and 9), but NaCl did not show any significant effect on the formation of this stop product (Figure 3B, lanes 5 and 6). The different effects of KCl and NaCl indicate that the KCl-specific block to DNA synthesis is not due to general effects of alkali ions. In the presence of 100 mM KCl, two additional stop products (3′-end and 5′-end) were produced at A38 and G25 (Figure 3B, lane 9), suggesting that the human PDGFR-β Pu38-mer has the capacity to form multiple intramolecular G-quadruplex structures that are preferentially stabilized by KCl. The stop product at the 3′-end includes a 5′-GGA tract, suggesting that the neighboring GGGAGGG sequence could form a stable double-chain reverse structure with a one-base loop (*33*) that is able to stabilize this species. The G-quadruplex structure causing the arrest site at G34 is the major G-quadruplex structure and is remarkably stable, since it produces an arrest product in the *Taq* polymerase stop assay even in the absence of KCl.

DMS Footprinting Reveals a Complex Pattern in Which Guanine Runs 4 and 5 Are Protected from Cleavage. The formation of a G-quadruplex can be determined by DMS footprinting patterns since N7 of guanine in a G-tetrad is protected from DMS methylation, in contrast to single-stranded or duplex DNA (*49*). The G-rich strand of the NHE has the potential to form multiple G-quadruplexes by using different

combinations of G-tracts within the seven runs of two or more guanines. To determine the major G-quadruplex structure in formation of the G-quadruplex, DMS footprinting was conducted in the absence and presence of 140 mM KCl (compare lanes 3 and 4 of Figure 3C). The DMS-protected and unprotected guanines are shown by empty and filled circles, respectively, while partially protected sites are shown by half- or quarter-filled circles. Guanine runs are numbered 1−7 on the left side of this gel. An unusual feature of the DMS cleavage pattern is that single guanines are protected in guanine runs 2 and 3, and there is complete protection of guanine runs 4 and 5, which consist of four and two consecutive guanines, respectively. Partial protection of most of the bases in guanine runs 6 and 7 further confirms the complexity of the G-quadruplexes formed by the PDGFR-β NHE. This DMS footprinting pattern is presumably a composite of three or more different G-quadruplexes.

Stabilization of the G-Quadruplex in the NHE with Small Molecules. Several studies have shown that certain small molecules can modulate gene transcription by stabilizing the biologically relevant G-quadruplexes formed in gene promoters (*20*−*23*, *30*−*33*). Therefore, in a reaction system without addition of any NaCl or KCl, we used the *Taq* polymerase stop assay to evaluate the abilities of three well-known G-quadruplex-interactive agents, TMPyP4, telomestatin, and Se2SAP (Figure 4A), to stabilize the G-quadruplexes in the NHE. TMPyP2, a positional isomer of TMPyP4 that lacks the ability to bind to G-quadruplex structures (*50*), served as the negative control in our studies. The results in Figure 4B (lanes 5−9) show that TMPyP2 has a negligible effect on the formation of stop products; however, upon addition of G-quadruplex-interactive agents to the mixture, four premature primer extension products were produced: stop products 5′-end, mid-5′, mid-3′, and 3′-end. The mid-5′ stop product was not detected in the absence of drugs (see Figure 3B). When the concentration of drugs was 0.5 μM, TMPyP4 and Se2SAP preferentially stabilized stop products 5′-end and mid-3′, which correspond to the arrest sites at G34 and G25 in the NHE Pu38-mer, respectively (Figure 4B, lanes 12 and 22). When the drug concentration was ≥1.0 μM, TMPyP4 bound to the duplex DNA (Figure 4B, lanes 13 and 14). Telomestatin stabilized all four premature stop products at a drug concentration of 0.5 μM. However, telomestatin preferentially stabilized the G-quadruplex structures associated with stop products 5′-end, mid-5′, and 3′-end (G25, G30, and A38, respectively) (Figure 3B, lane 17) at 0.5 μM and the major stop product 3′-end (A38) at 1 μM (Figure 4B, lane 18), which is a pattern different from that of TMPyP4 and Se2SAP. A graphical comparison of the relative intensities of the arrest products for telomestatin and Se2SAP at concentrations of 0.5 and 1.0 μM is shown in Figure 4C. Overall, these data show that telomestatin has a pattern of stop product stabilization different from that of TMPyP4 and Se2SAP.

Telomestatin Produces a Dose-Dependent Repression of Luciferase Expression Mediated by the Human PDGFR-β Promoter and PDGFR-β Expression in Daoy Cells. To directly assess the specific biological effects of G-quadruplex-interactive agents on human PDGFR-β promoter activity, Daoy cells were cotransfected with plasmids pGL-B and pRL-TK (internal control), which then were treated with incremental concentrations of TMPyP2, TMPyP4, Se2SAP, and telomestatin. As anticipated, TMPyP2 did not show any significant effect on the promoter activity of pGL-B (Figure 4A). However, TMPyP4, Se2SAP, and telomestatin produced either biphasic (TMPyP4

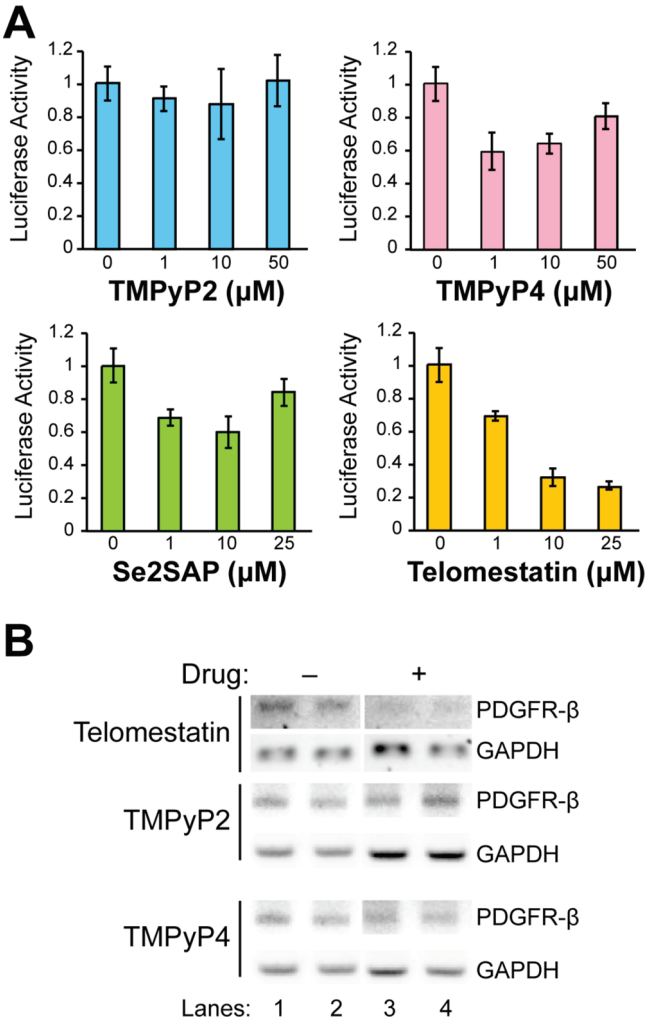

FIGURE 5: (A) Determination of the effects of G-quadruplex-interactive agents on the transcriptional activity of the human PDGFR-β basal promoter containing the NHE determined by the dual luciferase assay. The effects of TMPyP2, TMPyP4, Se2SAP, and telomestatin on the human PDGFR-β basal promoter activity are shown as the comparative firefly luciferase expression (firefly/Renilla) in each histogram. The values are the averages of three independent experiments. Error bars are the standard error. (B) Effect of telomestatin, TMPyP2, and TMPyP4 on mRNA levels of human PDGFR-β and GAPDH in Daoy cells. mRNA levels were measured in the absence or presence of telomestatin (1 μM), TMPyP2 (199 μM), or TMPyP4 (100 μM). Lanes 1 and 2 lack drugs, and lanes 3 and 4 include drugs. GAPDH was used as the control in each case. Data are representative of biological replicants at 24 h.

and Se2SAP) or a more typical dose-dependent inhibition (telomestatin) (Figure 5A) of the promoter activity of human PDGFR-β. In the absence of additional data about the function of the different G-quadruplexes in the PDGFR-β promoter, it is difficult to rationalize the biphasic effects of TMPyP4 and Se2SAP, but this is suggestive of a more complex role for the different G-quadruplexes in the control of gene expression. Most significantly, telomestatin reduced human PDGFR-β promoter activity by ~70% of the control at a concentration of 25 μM (Figure 5A). This latter result prompted us to determine the effect of telomestatin on human PDGFR-β transcription in human cancer cells.

Overexpression of PDGFR-β has been observed in medulloblastoma cells (*51*, *52*). Indeed, we confirmed that the level of expression of PDGFR-β in a medulloblastoma cell line (Daoy) is higher than that in normal tissue and in certain cancer cell lines,

such as HPDE-6 and Mia PaCa-2 (unpublished results). To directly assess the effect of telomestatin on the inhibition of human PDGFR-β transcription, we used semiquantitative reverse transcriptase polymerase chain reaction to analyze the change in PDGFR-β mRNA levels in telomestatin-treated Daoy cells. In triplicate experiments, Daoy cells that were treated with telomestatin, TMPyP2, and TMPyP4 for 24 h showed reproducible effects on PDGFR-β mRNA levels (Figure 5B). At a concentration of 1.0 μM, telomestatin markedly inhibited PDGFR-β expression in Daoy cells (Figure 5B, lanes 3 and 4), without affecting GAPDH expression. In contrast, there was no significant effect observed with either TMPyP2 or TMPyP4, mimicking those effects shown in Figure 5A. This result is consistent with the previous luciferase assay (Figure 5A) showing that telomestatin mediates its transcriptional inhibitory effect on human PDGFR-β transcription by specifically stabilizing one or more of the G-quadruplex structures formed in the NHE. The large differences in concentrations of telomestatin required for suppression of gene expression in panels A and B of Figure 5 are due to multiple copies of the plasmid in the experiment shown in panel A. We estimate that there are $\sim 4 \times 10^5$ plasmid copies following transfection.

DISCUSSION

Aberrant expression of PDGFR-β has been observed in several malignancies, such as dermatofibrosarcoma, glioblastoma, endocrine pancreatic tumor, and medulloblastoma (*4*−*7*, *51*−*53*). To cast light on the mechanisms that control PDGFR-β transcription, we have cloned and characterized the first functional promoter of the human PDGFR-β gene. Our studies show that the human PDGFR-β promoter does not have a TATA box. Two transcriptional start sites have been identified in the human PDGFR-β promoter. This observation is in accordance with numerous reports indicating that TATA box−less promoters usually drive the initiation of mRNA transcription from multiple sites (*54*, *55*). The human PDGFR-β promoter has a low level of sequence identity with the mouse PDGF-β promoter (*10*−*12*). Numerous studies have shown that Sp1, NF-Y, c-Myc, p73α, and p53 are involved in the regulation of mouse PDGFR-β promoter activity (*12*−*19*). The same (Sp1 and NF-Y) but also different (AP-1) consensus transcription factor binding sites are also found in the human PDGFR-β promoter. The CAAT box and the NHE located in the proximal promoter region of human PDGFR-β are predicted to be essential elements for human PDGFR-β transcription. However, the biological roles of some of these putative *cis* elements in the regulation of human PDGFR-β transcription still need to be determined.

The hypersensitivity to S1 nuclease of the human PDGFR-β polypurine/polypyrimidine region, NHE (base pairs −158 to 139), indicates that the NHE can adopt a non-B-DNA conformation in supercoiled plasmids. The S1-hypersensitive sites are localized predominantly on the C-rich stand of the human PDGFR-β NHE, and the complementary G-rich strand is resistant to S1 nuclease, suggesting that the G-rich strand of the NHE forms an unusual DNA structure, such as a G-quadruplex structure, and the C-rich strand assumes a partially single-stranded loop in supercoiled plasmids. Our studies show that G-quadruplex-forming regions in the proximal promoter of c-Myc and VEGF are also sensitive to nucleases and can form a G-quadruplex structure in supercoiled plasmids (*56*). It has been shown that the transcription-induced negative superhelicity in the c-Myc promoter plays a critical role in driving the interconversion between duplex and non-B-form conformations and, by implication, in other promoters having NHEs (*56*−*59*). Furthermore, the DMS footprinting and *Taq* polymerase stop assays show that the G-rich strand of the human PDGFR-β NHE can form stable G-quadruplex structures under physiological conditions. Along with the compelling observation from the Levens group that transcriptionally induced negative superhelicity can induce unwound regions of DNA (*58*), our studies on c-Myc using supercoiled plasmids, which also mimic the effect of transcriptionally induced negative superhelicity, further suggest that the G-quadruplex structures can be generated under negative superhelical stress in the c-Myc promoter and regulate its transcription. Analogously, in the polypurine/polypyrimidine regions of gene promoters such as VEGF and PDGFR-β, G-quadruplexes may play a more general role in the control of gene expression (*60*).

There is an intriguing relationship between the different patterns and potencies of PDGFR-β transcriptional repression by telomestatin versus Se2SAP and TMPyP4 (see Figure 5A) and the hierarchy of binding of these ligands to the different G-quadruplexes as determined by the polymerase stop assay (Figure 4B). Telomestatin shows a clear dose dependency for inhibition of luciferase activity in contrast to the effects of TMPyP4 and Se2SAP (Figure 5A). These contrasting effects of telomestatin versus TMPyP4 are also found on PDGFR-β expression levels in Daoy cells (Figure 5B). The KCl dependency experiment (Figure 3B) shows a clear preference for the G-quadruplex corresponding to stop product mid-3′, and the same stop product is favored by Se2SAP and TMPyP4. In contrast, telomestatin favors stop products 5′-end, mid-5′, and 3′-end, all of which are less favored than the stop product produced by Se2SAP and TMPyP4. Thus, telomestatin stabilizes the 3′-end and mid-5′ G-quadruplexes that are not favored by KCl or the other G-quadruplex-interactive compounds. For promoters such as c-Myc, where there is one predominant G-quadruplex, the repression effects of the G-quadruplexes can be assessed by simple mutational experiments (*61*). However, it is unfortunately not so for the PDGFR-β system. This conclusion is based on the differential effects of drugs (see Figure 5B) on PDGFR-β expression. Indeed, we have already designed a series of experiments to provide this type of data. However, because there are four overlapping G-quadruplexes, with highly likely different effects on gene expression, a set of plasmid inserts containing different combinations of guanine runs that form each of the defined G-quadruplexes and one- and two-base mutations of the full-length sequence are required to fully address this question. In subsequent experiments, a structurally distinct group of G-quadruplex-interactive compounds also showed differential effects dependent on G-quadruplex selectivity in this same promoter region. Therefore, it would appear that drug stabilization of different G-quadruplexes has differential effects on PDGFR-β gene expression. It is likely that the differential binding of telomestatin and Se2SAP to G-quadruplexes associated with different stop products is dependent on the heterogeneity of the folding patterns, loop sizes, and capping structures within these structures. These different ligands may be mimicking the effect of natural recognition elements, such as transcriptional factors, which can also differentially regulate PDGFR-β gene expression. Compelling data show that intramolecular G-quadruplexes that form within the promoters of some oncogenes, such as c-Myc, PDGF-A, VEGF, c-Kit-1, c-Kit-2, hTERT, and KRAS, and small molecules that bind to these G-quadruplexes

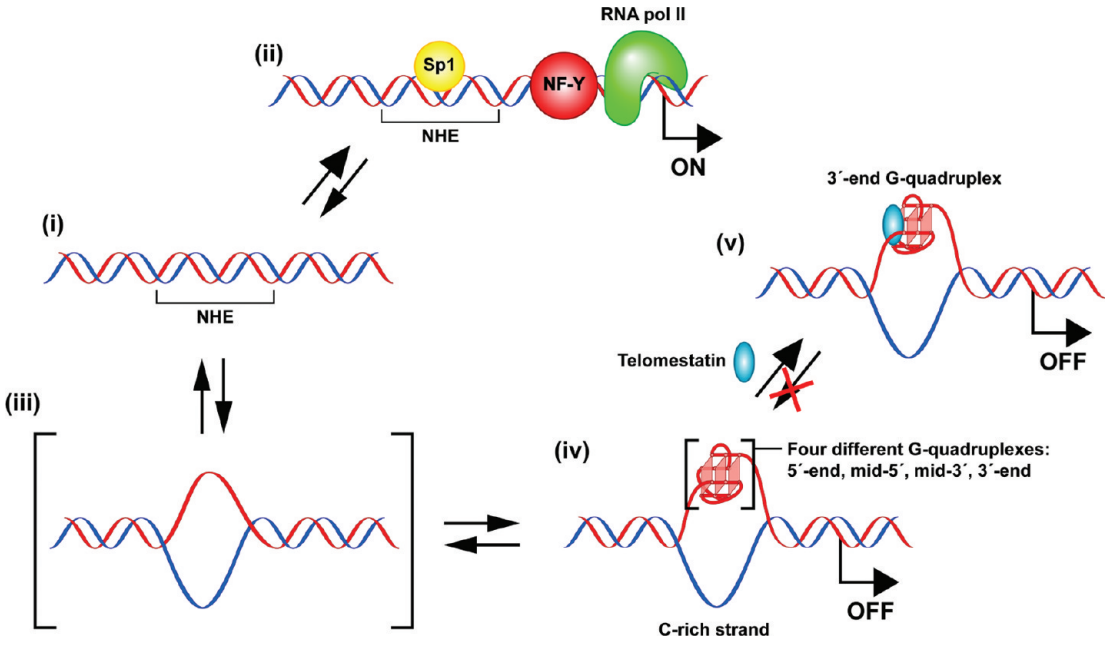

FIGURE 6: Model for the activation and repression of human PDGFR-β gene transcription in supercoiled DNA, involving the conversion of the duplex species (i) to the transcriptionally active species (ii). Sp1 and NF-Y are double-stranded DNA binding proteins involved in transcriptional activation of the NHE in the promoter. The duplex species (i), under negative superhelicity, can be converted to the various quadruplex-containing species (5′-end, mid-5′, mid-3′, and 3′-end) (iv) via the single-stranded species (iii). Interaction of the G-quadruplex structure (3′-end) in the NHE with telomestatin stabilizes the gene-off form to maintain transcriptional repression (v).

have been shown to inhibit transcriptional activation (*20*−*23*, *30*−*34*, *61*, *62*). Here, we demonstrate that the G-quadruplex formed in the human PDGFR-β NHE is a negative regulator and can be stabilized by G-quadruplex-interactive agents to cause transcriptional repression of PDGFR-β. This method of repressing PDGFR-β transcription is an alternative approach to targeting the PDGFR-β pathway and may be useful in treating drug-resistant tumors that are caused by mutation of the PDGFR-β kinase.

One generic characteristic of the G-quadruplex-forming regions in the oncogene promoters is that these regions also contain consensus binding sites for Sp1, which is a key player in the regulation of gene transcription (*33*, *63*−*67*). Therefore, it is not surprising that we also identified a conserved Sp1 binding site within the NHE of the human PDGFR-β promoter. As has been correctly pointed out, Sp1 consensus binding sites and G-quadruplex-forming elements are often coincident (*67*). However, rather than interpreting this as an argument against the biological relevance of G-quadruplexes in mediating a role in the control of gene expression, we suggest that this provides a gene-specific way of eliminating a ubiquitous transcription factor like Sp1 from promoter regions that are actively undergoing transcription.

On the basis of this new insight into the human PDGFR-β promoter and previous studies on c-Myc and PDGF-A promoters, we propose a model in which transcription factor Sp1 and the G-quadruplexes derived from the purine strand of the NHE are involved in the activation and repression of PDGFR-β transcription, respectively (Figure 6). In this model, the active transcriptional form (ii) is in equilibrium with the different G-quadruplex forms (5′-end, mid-5′, mid-3′, and 3′-end) (iv) via the single-stranded intermediate form (iii). Sp1 binds to the duplex conformation of the NHE, and the transcriptional machinery is recruited to the proximal promoter region, initiating the transcription (i to ii). However, as transcription proceeds, the transcriptionally generated negative superhelical torsion can topologically convert the duplex NHE region (i and ii) via a single-stranded conformation (iii) and displace the Sp1 that may lead to down-regulation of transcription. As the transcriptionally generated negative superhelicity increases, the polypurine/polypyrimidine region of the PDGFR-β promoter can be energetically driven to form different secondary DNA structures such as G-quadruplexes (5′-end, mid-5′, mid-3′, and 3′-end). The dynamic interconversion between duplex and G-quadruplex conformations provides a real-time transcriptional feedback mechanism for the regulation of human PDGFR-β transcription. Furthermore, one of the G-quadruplex forms of the NHE (3′-end) can be frozen in the presence of telomestatin, which shifts the equilibrium away from the active transcription form (iv to v). The precise details of the structures of the different G-quadruplexes and their complexes with telomestatin and TMPyP4 are under investigation in our laboratory and reveal the diversity of the G-quadruplex folding patterns and structures. These studies are ongoing, as is the development of more druglike molecules for potential clinical use.

ACKNOWLEDGMENT

We thank Daniel Von Hoff for his advice on the initiation of the human PDGFR-β promoter project and Tao Li (Department of Pediatrics and Medicine, University of Arizona) for technical support in cloning the human PDGFR-β promoter. We also thank Kazuo Shin-ya (University of Tokyo) for providing the telomestatin. We are grateful to David Bishop for preparing, proofreading, and editing the final version of the manuscript and figures.

REFERENCES

1. Heldin, C. H., Eriksson, U., and Ostman, A. (2002) New members of the platelet-derived growth factor family of mitogens. *Arch. Biochem. Biophys. 398*, 284–290.
2. Betsholtz, C. (2003) Biology of platelet-derived growth factors in development. *Birth Defects Res., Part C 69*, 272–285.

3. Alvarez, R. H., Kantarjian, H. M., and Cortes, J. E. (2006) Biology of platelet-derived growth factor and its involvement in disease. *Mayo Clin. Proc. 81*, 1241–1257.
4. Pietras, K., Sjöblom, T., Rubin, K., Heldin, C. H., and Ostman, A. (2003) PDGF receptors as cancer drug targets. *Cancer Cell 3*, 439–443.
5. Yu, J., Ustach, C., and Kim, H. R. (2003) Platelet-derived growth factor signaling and human cancer. *J. Biochem. Mol. Biol. 36*, 49–59.
6. Pietras, K., Ostman, A., Sjöquist, M., Buchdunger, E., Reed, R. K., Heldin, C. H., and Rubin, K. (2001) Inhibition of platelet-derived growth factor receptors reduces interstitial hypertension and increases transcapillary transport in tumors. *Cancer Res. 61*, 2929–2934.
7. Ostman, A., and Heldin, C. H. (2007) PDGF receptors as targets in tumor treatment. *Adv. Cancer Res. 97*, 247–274.
8. Pietras, K., Rubin, K., Sjöblom, T., Buchdunger, E., Sjöquist, M., Heldin, C. H., and Ostman, A. (2002) Inhibition of PDGF receptor signaling in tumor stroma enhances antitumor effect of chemotherapy. *Cancer Res. 62*, 5476–5484.
9. Furuhashi, M., Sjöblom, T., Abramsson, A., Ellingsen, J., Micke, P., Li, H., Bergsten-Folestad, E., Eriksson, U., Heuchel, R., Betsholtz, C., Heldin, C. H., and Ostman, A. (2004) Platelet-derived growth factor production by B16 melanoma cells leads to increased pericyte abundance in tumors and an associated increase in tumor growth rate. *Cancer Res. 64*, 2725–2733.
10. Ballagi, A. E., Ishizaki, A., Nehlin, J. O., and Funa, K. (1995) Isolation and characterization of the mouse PDGF β-receptor promoter. *Biochem. Biophys. Res. Commun. 210*, 165–173.
11. Shinbrot, E., Liao, X., and Williams, L. T. (1997) Isolation and characterization of the platelet-derived growth factor β receptor promoter. *Dev. Dyn. 208*, 211–219.
12. Kitami, Y., Fukuoka, T., Okura, T., Takata, Y., Maguchi, M., Igase, M., Kohara, K., and Hiwada, K. (1998) Molecular structure and function of rat platelet-derived growth factor β-receptor gene promoter. *J. Hypertens. 16*, 437–445.
13. Funa, K., and Uramoto, H. (2003) Regulatory mechanisms for the expression and activity of platelet-derived growth factor receptor. *Acta Biochim. Pol. 50*, 647–658.
14. Molander, C., Hackzell, A., Ohta, M., Izumi, H., and Funa, K. (2001) Sp1 is a key regulator of the PDGF β-receptor transcription. *Mol. Biol. Rep. 28*, 223–233.
15. Izumi, H., Molander, C., Penn, L. Z., Ishisaki, A., Kohno, K., and Funa, K. (2001) Mechanism for the transcriptional repression by c-Myc on PDGF β-receptor. *J. Cell Sci. 114* (Part 8), 1533–1544.
16. Mao, D. Y., Barsyte-Lovejoy, D., Ho, C. S., Watson, J. D., Stojanova, A., and Penn, L. Z. (2004) Promoter-binding and repression of PDGFRB by c-Myc are separable activities. *Nucleic Acids Res. 32*, 3462–3468.
17. Uramoto, H., Hackzell, A., Wetterskog, D., Ballági, A., Izumi, H., and Funa, K. (2004) pRb, Myc and p53 are critically involved in SV40 large T antigen repression of PDGF β-receptor transcription. *J. Cell Sci. 117* (Part 17), 3855–3865.
18. Uramoto, H., Wetterskog, D., Hackzell, A., Matsumoto, Y., and Funa, K. (2004) p73 competes with co-activators and recruits histone deacetylase to NF-Y in the repression of PDGF β-receptor. *J. Cell Sci. 117* (Part 22), 5323–5331.
19. Silva, R. L., Thornton, J. D., Martin, A. C., Rehg, J. E., Bertwistle, D., Zindy, F., and Skapek, S. X. (2005) Arf-dependent regulation of Pdgf signaling in perivascular cells in the developing mouse eye. *EMBO J. 24*, 2803–2814.
20. Hurley, L. H., Von Hoff, D. D., Siddiqui-Jain, A., and Yang, D. (2006) Drug targeting of the c-MYC promoter to repress gene expression via a G-quadruplex silencer element. *Semin. Oncol. 33*, 498–512.
21. Seenisamy, J., Rezler, E. M., Powell, T. J., Tye, D., Gokhale, V., Joshi, C. S., Siddiqui-Jain, A., and Hurley, L. H. (2004) The dynamic character of the G-quadruplex element in the c-Myc promoter and modification by TMPyP4. *J. Am. Chem. Soc. 126*, 8702–8709.
22. Dexheimer, T. S., Sun, D., and Hurley, L. H. (2006) Deconvoluting the structural and drug-recognition complexity of the G-quadruplex-forming region upstream of the bcl-2 P1 promoter. *J. Am. Chem. Soc. 128*, 5404–5415.
23. Sun, D., Guo, K., Rusche, J. J., and Hurley, L. H. (2006) Facilitation of a structural transition in the polypurine/polypyrimidine tract within the proximal promoter region of the human VEGF gene by the presence of potassium and G-quadruplex-interactive agents. *Nucleic Acids Res. 33*, 6070–6080.
24. De Armond, R., Wood, S., Sun, D., Hurley, L. H., and Ebbinghaus, S. W. (2005) Evidence for the presence of a guanine quadruplex forming region within a polypurine tract of the hypoxia inducible factor 1α promoter. *Biochemistry 44*, 16341–16350.
25. Guo, K., Pourpak, A., Beetz-Rogers, K., Gokhale, V., Sun, D., and Hurley, L. H. (2007) Formation of pseudosymmetrical G-quadruplex and i-motif structures in the proximal promoter region of the RET oncogene. *J. Am. Chem. Soc. 129*, 10220–10228.
26. Todd, A. K., Haider, S. M., Parkinson, G. N., and Neidle, S. (2007) Sequence occurrence and structural uniqueness of a G-quadruplex in the human c-kit promoter. *Nucleic Acids Res. 35*, 5799–5808.
27. Bejugam, M., Sewitz, S., Shirude, P. S., Rodriguez, R., Shahid, R., and Balasubramanian, S. (2007) Trisubstituted isoalloxazines as a new class of G-quadruplex binding ligands: Small molecule regulation of c-kit oncogene expression. *J. Am. Chem. Soc. 129*, 12926–12927.
28. Phan, A. T., Kuryavyi, V., Burge, S., Neidle, S., and Patel, D. J. (2007) Structure of an unprecedented G-quadruplex scaffold in the human c-kit promoter. *J. Am. Chem. Soc. 129*, 4386–4392.
29. Palumbo, S. L., Memmott, R. M., Uribe, D. J., Krotova-Khan, Y., Hurley, L. H., and Ebbinghaus, S. W. (2008) A novel G-quadruplex forming GGA repeat region in the c-myb promoter is a critical regulator of promoter activity. *Nucleic Acids Res. 36*, 1755–1769.
30. Cogoi, S., and Xodo, L. E. (2006) G-quadruplex formation within the promoter of the KRAS proto-oncogene and its effect on transcription. *Nucleic Acids Res. 34*, 2536–2549.
31. Qin, Y., Rezler, E. M., Gokhale, V., Sun, D., and Hurley, L. H. (2007) Characterization of the G-quadruplexes in the duplex nuclease hypersensitive element of the PDGF-A promoter and modulation of PDGF-A promoter activity by TMPyP4. *Nucleic Acids Res. 35*, 7698–7713.
32. Palumbo, S. L., Ebbinghaus, S. W., and Hurley, L. H. (2009) Formation of a unique end-to-end stacked pair of G-quadruplexes in the hTERT core promoter with implications for inhibition of telomerase by G-quadruplex-interactive ligands. *J. Am. Chem. Soc. 131*, 10878–10891.
33. Qin, Y., and Hurley, L. H. (2009) Structures, folding patterns, and functions of intramolecular DNA G-quadruplexes found in eukaryotic promoter regions. *Biochimie 90*, 1149–1171.
34. Hsu, S. T., Varnai, P., Bugaut, A., Reszka, A. P., Neidle, S., and Balasubramanian, S. (2009) A G-rich sequence within the *c-kit* oncogene promoter forms a parallel G-quadruplex having asymmetric G-tetrad dynamics. *J. Am. Chem. Soc. 131*, 13399–13409.
35. Gomez, D., O'Donohue, M. F., Wenner, T., Douarre, C., Macadré, J., Koebel, P., Giraud-Panis, M. J., Kaplan, H., Kolkes, A., Shin-ya, K., and Riou, J. F. (2006) The G-quadruplex ligand telomestatin inhibits POT1 binding to telomeric sequences in vitro and induces GFP-POT1 dissociation from telomeres in human cells. *Cancer Res. 66*, 6908–6912.
36. Li, T., Walsh, J. R., Ghishan, F. K., and Bai, L. (2004) Molecular cloning and characterization of a human urate transporter (hURAT1) gene promoter. *Biochim. Biophys. Acta 1681*, 53–58.
37. Han, H., Hurley, L. H., and Salazar, M. (1999) A DNA polymerase stop assay for G-quadruplex-interactive compounds. *Nucleic Acids Res. 27*, 537–542.
38. Nemoto, E., Shimonishi, M., Nitta, Y., and Shimauchi, H. (2004) The involvement of platelet-derived growth factor receptors and insulin-like growth factor-I receptors signaling during mineralized nodule formation by human periodontal ligament cells. *J. Periodontal Res. 39*, 388–397.
39. Provencio, I., Rodriguez, I. R., Jiang, G., Hayes, W. P., Moreira, E. F., and Rollag, M. D. (2000) A novel human opsin in the inner retina. *J. Neurosci. 20*, 600–605.
40. Gronwald, R. G., Grant, F. J., Haldeman, B. A., Hart, C. E., O'Hara, P. J., Hagen, F. S., Ross, R., Bowen-Pope, D. F., and Murray, M. J. (1988) Cloning and expression of a cDNA coding for the human platelet-derived growth factor receptor: Evidence for more than one receptor class. *Proc. Natl. Acad. Sci. U.S.A. 85*, 3435–3439.
41. Jones, A. V., and Cross, N. C. (2004) Oncogenic derivatives of platelet-derived growth factor receptors. *Cell. Mol. Life Sci. 61*, 2912–2923.
42. Benjamin, L. (2004) DNase hypersensitive sites change chromatin structure. In Genes VII (Benjamin, L., Ed.) pp 593−597, Oxford University Press, New York.
43. Elgin, S. C. (1981) DNAase I-hypersensitive sites of chromatin. *Cell 27*, 413–415.
44. Larsen, A., and Weintraub, H. (1982) An altered DNA conformation detected by S1 nuclease occurs at specific regions in active chick globin chromatin. *Cell 29*, 609–622.
45. Maurizot, J. C. (2000) Circular dichroism of nucleic acids: Nonclassical conformations and modified oligonucleotides. In Circular Dichroism: Principles and Applications (Berova, N., Nakanishi, K., and Woody, R. W., Eds.) pp 719−736, Wiley-VCH, New York.

46. Dai, J., Chen, D., Jones, R. A., Hurley, L. H., and Yang, D. (2006) NMR solution structure of the major G-quadruplex structure formed in the human BCL2 promoter region. *Nucleic Acids Res. 34*, 5133–5144.
47. Hud, N. V., Smith, F. W., Anet, F. A., and Feigon, J. (1996) The selectivity for K^+ versus Na^+ in DNA quadruplexes is dominated by relative free energies of hydration: A thermodynamic analysis by ^1H NMR. *Biochemistry 35*, 15383–15390.
48. Alberts, B. (2002) Internal organization of the cell. In Molecular Biological of the Cell (Alberts, B., Johnson, A., and Lewis, J., Eds.) pp 615−657, Garland Science, New York.
49. Vialas, C., Pratviel, G., and Meunier, B. (2000) Oxidative damage generated by an oxo-metalloporphyrin onto the human telomeric sequence. *Biochemistry 39*, 9514–9522.
50. Han, F. X., Wheelhouse, R. T., and Hurley, L. H. (1999) Interactions of TMPyP4 and TMPyP2 with quadruplex DNA. Structural basis for the differential effects on telomerase inhibition. *J. Am. Chem. Soc. 121*, 3561–3570.
51. MacDonald, T. J., Brown, K. M., LaFleur, B., Peterson, K., Lawlor, C., Chen, Y., Packer, R. J., Cogen, P., and Stephan, D. A. (2001) Expression profiling of medulloblastoma: PDGFRA and the RAS/MAPK pathway as therapeutic targets for metastatic disease. *Nat. Genet. 29*, 143–152.
52. Gilbertson, R. J., and Clifford, S. C. (2003) PDGFRB is overexpressed in metastatic medulloblastoma. *Nat. Genet. 35*, 197–198.
53. Fjällskog, M. L., Hessman, O., Eriksson, B., and Janson, E. T. (2007) Upregulated expression of PDGF receptor β in endocrine pancreatic tumors and metastases compared to normal endocrine pancreas. *Acta Oncol. 46*, 741–746.
54. Ince, T. A., and Scotto, K. W. (1995) A conserved downstream element defines a new class of RNA polymerase II promoters. *J. Biol. Chem. 270*, 30249–30252.
55. David, M. D., Bertoglio, J., and Pierre, J. (2003) Functional characterization of IL-13 receptor α2 gene promoter: A critical role of the transcription factor STAT6 for regulated expression. *Oncogene 22*, 3386–3394.
56. Sun, D., and Hurley, L. H. (2009) The importance of negative superhelicity in inducing the formation of G-quadruplex and i-motif structures in the c-Myc promoter: Implications for drug targeting and control of gene expression. *J. Med. Chem. 52*, 2863–2874.
57. Brooks, T. A., and Hurley, L. H. (2009) The role of supercoiling in transcriptional control of c-myc and its importance in molecular therapeutics. *Nat. Rev. Cancer 9*, 849–861.
58. Kouzine, F., Sanford, S., Elisha-Feil, Z., and Levens, D. (2008) The functional response of upstream DNA to dynamic supercoiling in vivo. *Nat. Struct. Mol. Biol. 15*, 46–54.
59. Lavelle, C. (2008) DNA torsional stress propagates through chromatin fiber and participates in transcriptional regulation. *Nat. Struct. Mol. Biol. 15*, 123–125.
60. Sun, D., Liu, W. J., Guo, K., Ebbinghaus, S., Gokhale, V., and Hurley, L. H. (2008) The proximal promoter region of the human vascular endothelial growth factor gene has a G-quadruplex structure that can be targeted by G-quadruplex-interactive agents. *Mol. Cancer Ther. 7*, 880–889.
61. Siddiqui-Jain, A., Grand, C. L., Bearss, D. J., and Hurley, L. H. (2002) Direct evidence for a G-quadruplex in a promoter region and its targeting with a small molecule to repress c-*MYC* transcription. *Proc. Natl. Acad. Sci. U.S.A. 99*, 11593–11598.
62. Gunaratnam, M., Swank, S., Haider, S. M., Galesa, K., Reszka, A. P., Beltran, M., Cuenca, F., Fletcher, J. A., and Neidle, S. (2009) Targeting human gastrointestinal stromal tumor cells with a quadruplex-binding small molecule. *J. Med. Chem. 52*, 3774–3783.
63. Miller, T. L., Jin, Y., Sun, J. M., Coutts, A. S., Murphy, L. C., and Davie, J. R. (1996) Analysis of human breast cancer nuclear proteins binding to the promoter elements of the c-myc gene. *J. Cell. Biochem. 60*, 560–571.
64. Silverman, E. S., Khachigian, L. M., Lindner, V., Williams, A. J., and Collins, T. (1997) Inducible PDGF A-chain transcription in smooth muscle cells is mediated by Egr-1 displacement of Sp1 and Sp3. *Am. J. Physiol. 273*, H1415–H1426.
65. Santra, M., Santra, S., Zhang, J., and Chopp, M. (2007) Ectopic decorin expression up-regulates VEGF expression in mouse cerebral endothelial cells via activation of the transcription factors Sp1, HIF1α, and Stat3. *J. Neurochem. 105*, 324–337.
66. Andrew, S. D., Delhanty, P. J., Mulligan, L. M., and Robinson, B. G. (2000) Sp1 and Sp3 transactivate the RET proto-oncogene promoter. *Gene 256*, 283–291.
67. Eddy, J., and Maizels, N. (2008) Conserved elements with potential to form polymorphic G-quadruplex structures in the first intron of human genes. *Nucleic Acids Res. 36*, 1321–1333.